

Dielectric Properties of Low-Firing $\text{Bi}_2\text{Mo}_2\text{O}_9$ Thick Films Screen Printed on Al Foils and Alumina Substrates

Weihong Liu, Hong Wang,[†] Di Zhou, and Kecheng Li

Electronic Materials Research Laboratory, Key Laboratory of the Ministry of Education, Xi'an Jiaotong University, Xi'an 710049, China

Low-firing $\text{Bi}_2\text{Mo}_2\text{O}_9$ thick films with a thickness of 15–20 μm were screen printed on Al foils and alumina substrates by screen-printing technology. The phase evolution, morphologies, and dielectric properties of the thick films were investigated. The thick films showed a pure $\text{Bi}_2\text{Mo}_2\text{O}_9$ phase at temperatures below 610°C. A mixture of Bi_2MoO_6 , $\text{Bi}_2\text{Mo}_3\text{O}_{12}$, and $\text{Bi}_2\text{Mo}_2\text{O}_9$ phases was found in the thick films sintered at 610°C and higher temperatures. The $\text{Bi}_2\text{Mo}_2\text{O}_9$ thick films on Al foils sintered at 645°C showed excellent dielectric properties with a relative permittivity of 38 and a dielectric loss of 0.7% at 5 MHz. At the microwave frequency range from 5 to 19 GHz, the $\text{Bi}_2\text{Mo}_2\text{O}_9$ thick films on alumina substrates sintered at 645°C had a relative permittivity of ~ 35 and $Q \times f$ of $\sim 12,500$ GHz. It indicates that the $\text{Bi}_2\text{Mo}_2\text{O}_9$ composition as potentially useful for low-temperature cofired ceramic using Al electrode.

I. Introduction

THE rapidly growing wireless industry requires high-performance dielectric materials for microwave device applications such as filters, duplexers, voltage-controlled oscillators, and antennas. The low-temperature cofired ceramic (LTCC) technology offers significant benefits over other established packaging technologies for high density, reliable RF, and fast digital applications requiring hermetical packaging and good thermal management.^{1–4} Microwave LTCC dielectric materials with low sintering temperature, high relative permittivity ϵ_r , low dielectric loss, and near-zero temperature coefficient of resonant frequency temperature coefficient (TCF) are needed to be cofired with low-loss, low-melting-point conductors such as Ag, Cu, Au, or Al.

Although there are many microwave dielectric compositions with high quality factor Q and high relative permittivity ϵ_r , their densification temperatures are typically $> 1000^\circ\text{C}$, such as $\text{ZnO-Nb}_2\text{O}_5$, $\text{Bi}(\text{Nb}, \text{Ta}, \text{Sb})\text{O}_4$, $\text{BaO-TiO}_2\text{-Nb}_2\text{O}_5$ system, $\text{Li}_2\text{O-Nb}_2\text{O}_5\text{-TiO}_2$ system, $(\text{Zr}, \text{Sn})\text{TiO}_4$, and $(\text{A}_1\text{A}_2)(\text{B}_1\text{B}_2)\text{O}_3$ complex perovskite system.⁵ To utilize these dielectric compositions in LTCC technology, it is required to lower their densification temperatures to $< 961^\circ\text{C}$ (melting point of Ag) because Ag is a typically used internal electrode in LTCC technology. To lower the sintering temperature, the addition of some sintering aids, such as V_2O_5 , CuO , and B_2O_3 , are normally used, which could lower the sintering temperature but also increase the dielectric loss ($\sim 1/Q$). Hence, more attention has been paid for seeking new dielectric compounds with intrinsically low sintering temperatures, which include materials in the following systems: $\text{Bi}_2\text{O}_3\text{-TeO}_2$, $\text{TiO}_2\text{-TeO}_2$, CaO-TeO_2 , BaO-TeO_2 binary

systems, $\text{BaO-TiO}_2\text{-TeO}_2$ ternary system, and $\text{Bi}_2\text{W}_2\text{O}_9$ systems.^{6–11}

Recently Zhou *et al.*¹² demonstrated that a single-phase $\text{Bi}_2\text{Mo}_2\text{O}_9$ could be sintered at a temperature of $\sim 620^\circ\text{C}$ and possessed excellent microwave dielectric properties. It has a relative permittivity ~ 38 , $Q \times f \sim 12,500$ GHz, and a TCF about $+31$ ppm/ $^\circ\text{C}$. In spite of their low sintering temperature and excellent dielectric properties, the application of the $\text{Bi}_2\text{Mo}_2\text{O}_9$ to LTCC technology has been limited because of its poor chemical compatibility with silver. This problem was also observed in BaTe_4O_9 and $\text{Zn}_2\text{Te}_3\text{O}_8$ -based ceramics, and has been overcome through the use of Al or gold electrodes.^{10,13,14} More extensive investigations have been carried out on $\text{Bi}_2\text{Mo}_2\text{O}_9$ ceramic and its compatibility with Al.¹⁵ The results of prototype MLCC by $\text{Bi}_2\text{Mo}_2\text{O}_9$ ceramic with Al paste as an internal electrode proved that Al can be used as an internal electrode for $\text{Bi}_2\text{Mo}_2\text{O}_9$ ceramic's application to multilayer devices.

In this work, the $\text{Bi}_2\text{Mo}_2\text{O}_9$ thick films were fabricated on Al foils and alumina substrates using screen-printing technology. The structure and dielectric properties of the thick films were investigated. The interaction between Al and $\text{Bi}_2\text{Mo}_2\text{O}_9$ was studied. The dielectric properties of the $\text{Bi}_2\text{Mo}_2\text{O}_9$ thick films on Al foils and alumina substrates were evaluated for the applications in LTCC microwave circuits.

II. Experimental Procedures

To synthesize the $\text{Bi}_2\text{Mo}_2\text{O}_9$ ceramic powder, Bi_2O_3 ($> 99\%$, Shu-Du Powders Co. Ltd., Chengdu, China) and MoO_3 ($> 99\%$, Fuchen Chemical Reagents, Tianjin, China) were used as the starting materials. A mixture of Bi_2O_3 and MoO_3 in a stoichiometric molar ratio of $\text{Bi}_2\text{Mo}_2\text{O}_9$ was ball milled for 4 h in a planetary mill (Nanjing Machine Factory, Nanjing, China) and calcined at 600°C . Experimental details, together with the properties of the synthesized material, are given in our previous work.¹² The calcined powders were ball milled again to obtain submicrometer-size powder appropriate for screen-printing technology.

The dried submicrometer-sized powder was mixed with an organic vehicle (ceramic powder: organic vehicle = 66.7:33.3 wt%) by stirring for about 1 h to form a paste for screen-printing technology. To test the dielectric properties of thick films and the interaction between $\text{Bi}_2\text{Mo}_2\text{O}_9$ and Al, Al (99%) foils are used as substrates. For testing the microwave dielectric properties of thick films, alumina (99%) substrates were used. The screen-printing process was repeated until the desired thickness was attained. Each layer of the thick films was preheated at 100°C for 10 min subsequently. Then, the thick films were sintered at temperatures ranging from 550° to 650°C for different dwell time in the furnace.

The phases of the deposited thick films were identified by X-ray diffraction with $\text{CuK}\alpha$ radiation (X-ray diffractometry, Rigaku D/MAX-2400, Tokyo, Japan). A scanning electron microscope (SEM, JSM-6460, JEOL, Tokyo, Japan), equipped with a Tracor-Northern energy-dispersive system (EDS) (Tokyo, Japan), was used for the microstructure analysis. For the

D. Lupascu—contributing editor

Manuscript No. 26699. Received September 15, 2009; approved February 4, 2010.

This work was supported by the National 973-project of China (2009CB623302), NSFC projects of China (10979035, 60871044, 50835007), and International S&T Cooperation Program of China (2009DFA51820).

[†]Author to whom correspondence should be addressed. e-mail: hwang@mail.xjtu.edu.cn

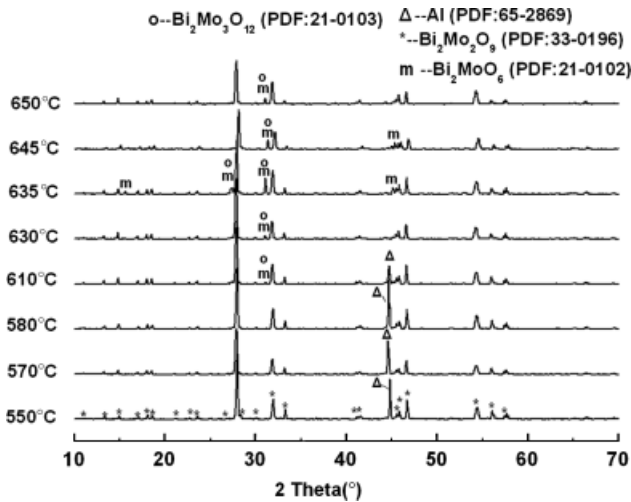


Fig. 1. X-ray diffraction patterns of $\text{Bi}_2\text{Mo}_2\text{O}_9$ thick films on Al foils under different sintering temperatures for 3 h (o—phase of $\text{Bi}_2\text{Mo}_3\text{O}_{12}$, Δ —phase of Al, *—phase of $\text{Bi}_2\text{Mo}_2\text{O}_9$, m—phase of Bi_2MoO_6).

low-frequency measurements of the thick films on Al foils, top electrodes with dimensions of 3.14 mm^2 were deposited by gold sputtering. The relative permittivity and dielectric losses were measured using a high-precision LCR meter (Agilent 4294A LCR meter, Agilent, Palo Alto, CA). The microwave dielectric properties of thick films on alumina substrates were measured by the split postresonator method¹⁶ with a vector network analyzer (8720ES, Agilent) and a temperature chamber (Delta 9023, Delta Design, Poway, CA). The $\text{TC}\epsilon$ (τ_ϵ) was calculated by the following formula:

$$\tau_\epsilon = \frac{\epsilon_{85} - \epsilon_{25}}{\epsilon_{25} \times (85 - 25)} \quad (1)$$

where ϵ_{85} and ϵ_{25} were the relative permittivity at 85° and 25°C, respectively.

III. Results and Discussion

The X-ray diffraction patterns of $\text{Bi}_2\text{Mo}_2\text{O}_9$ thick films on Al foils and alumina substrates sintered at temperatures of 550°–650°C for 3 h are shown in Figs. 1 and 2, respectively. The

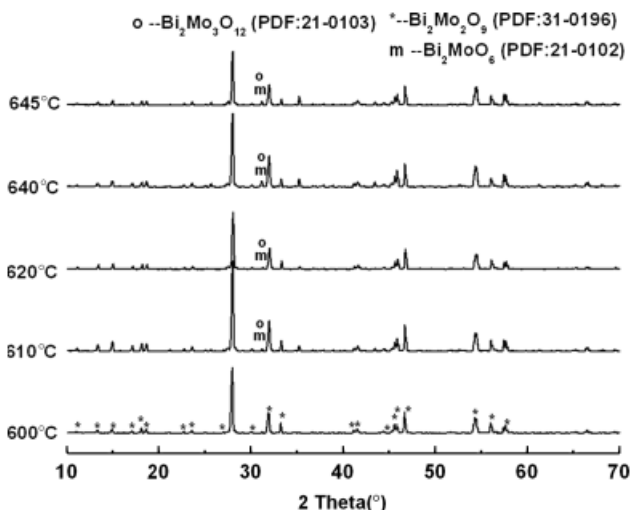


Fig. 2. X-ray diffraction patterns of $\text{Bi}_2\text{Mo}_2\text{O}_9$ thick films on alumina substrates sintered at different temperatures for 3 h (o—phase of $\text{Bi}_2\text{Mo}_3\text{O}_{12}$, *—phase of $\text{Bi}_2\text{Mo}_2\text{O}_9$, m—phase of Bi_2MoO_6).

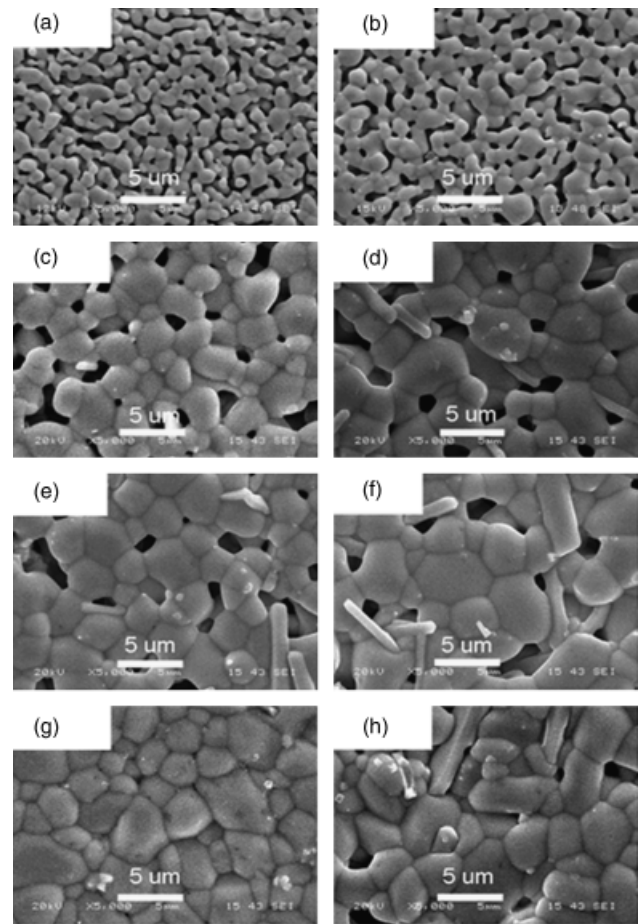


Fig. 3. Scanning electron microscope photos of surface morphologies of $\text{Bi}_2\text{Mo}_2\text{O}_9$ thick films on Al foils sintered at (a) 550°C, (b) 580°C, (c) 610°C, (d) 620°C, (e) 630°C, (f) 635°C, (g) 645°C, and (h) 650°C for 3 h.

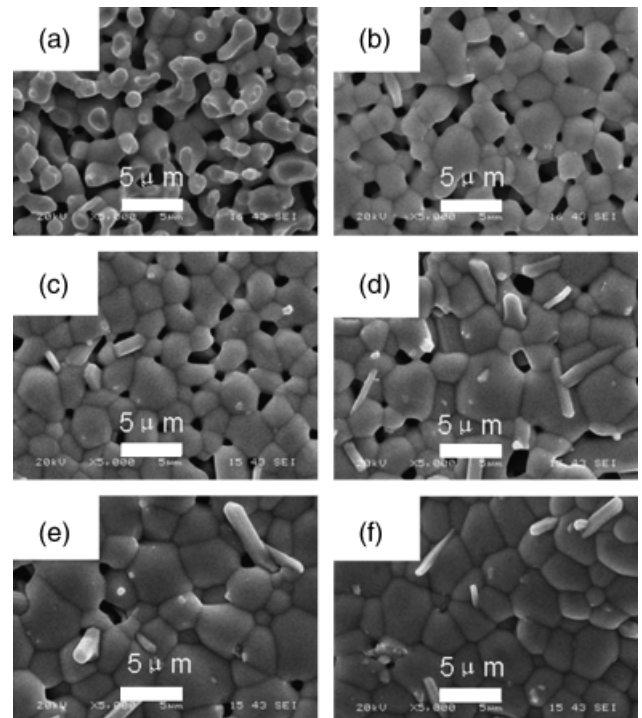


Fig. 4. Scanning electron microscope photos of surface morphologies of $\text{Bi}_2\text{Mo}_2\text{O}_9$ thick films on alumina substrates sintered at (a) 550°C, (b) 580°C, (c) 610°C, (d) 630°C, (e) 635°C, and (f) 645°C for 3 h.

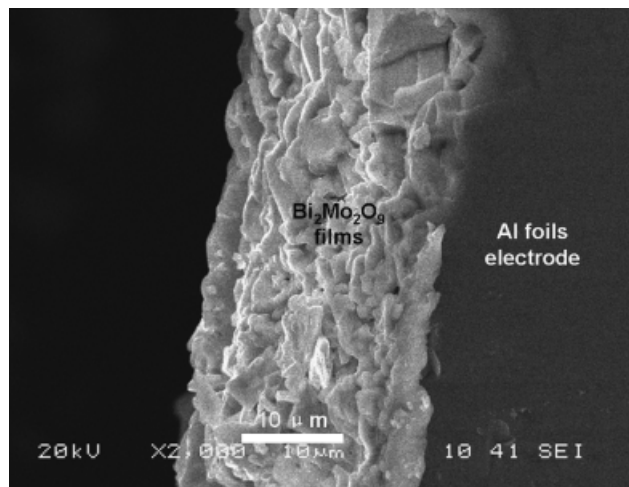


Fig. 5. Cross-sectional scanning electron microscope photo of the co-fired $\text{Bi}_2\text{Mo}_2\text{O}_9/\text{Al}$ sample sintered at 645°C for 3 h in air.

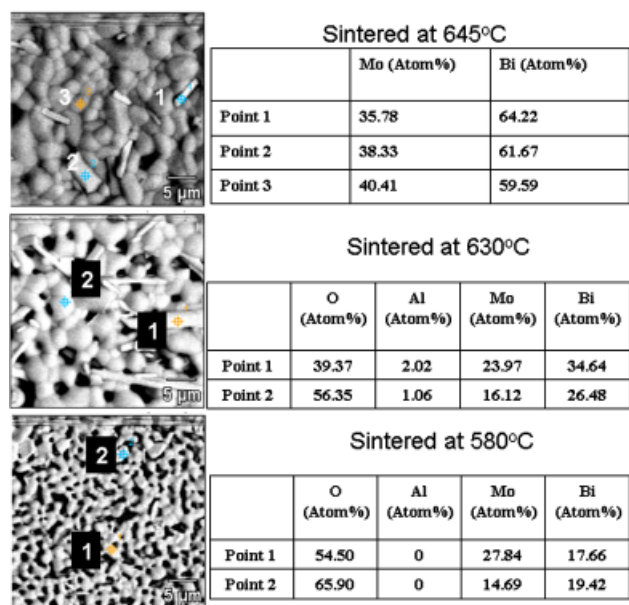


Fig. 6. Energy-dispersive system result of $\text{Bi}_2\text{Mo}_2\text{O}_9$ thick film on Al foils sintered at 645° , 630° , and 580°C for 3 h.

diffraction peaks of the thick films sintered below 610°C can be indexed as single phase $\text{Bi}_2\text{Mo}_2\text{O}_9$. A small amount of the Bi_2MoO_6 and $\text{Bi}_2\text{Mo}_3\text{O}_{12}$ phase is found to be formed in the thick films sintered at 610°C and higher temperatures. These results are different from that of the bulk $\text{Bi}_2\text{Mo}_2\text{O}_9$ ceramics. According to our previous work,¹² when the sintering temperature is below 645°C , all peaks are indexed as a single phase $\text{Bi}_2\text{Mo}_2\text{O}_9$, and no secondary phase of Bi_2MoO_6 or $\text{Bi}_2\text{Mo}_3\text{O}_{12}$ is observed in the bulk ceramics. Hence, the emergence of the

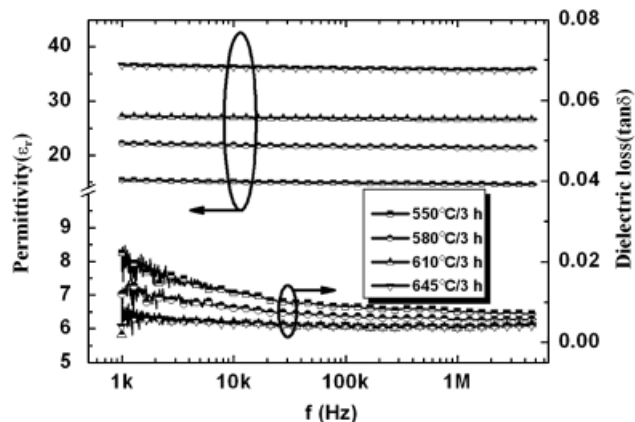


Fig. 8. Dielectric properties of $\text{Bi}_2\text{Mo}_2\text{O}_9$ thick films on Al foils sintered at different temperatures.

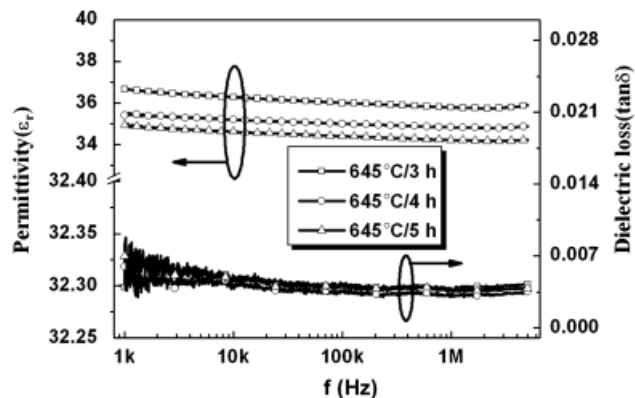


Fig. 9. Dielectric properties of $\text{Bi}_2\text{Mo}_2\text{O}_9$ thick films on Al foils sintered at 645°C for different dwell time.

secondary phases in the thick films is ascribed to the interaction between the substrates (Al and alumina) and $\text{Bi}_2\text{Mo}_2\text{O}_9$ during the sintering process. With the emergence of a small amount of the Bi_2MoO_6 and $\text{Bi}_2\text{Mo}_3\text{O}_{12}$ phase in the thick films on Al foils sintered at 610°C , the Al diffraction peak became weak and then disappeared at higher temperatures. This means that the surface of the Al foil is probably oxidized to a layer of Al_2O_3 at 610°C and higher temperatures. Then, the Al^{3+} ions from the Al_2O_3 layer on the Al foils or Al_2O_3 substrates entered the $\text{Bi}_2\text{Mo}_2\text{O}_9$ lattice and partly occupied the sites of molybdenum to form the $\text{Bi}_2\text{Mo}_{2-2x}\text{Al}_{2x}\text{O}_{9-3x}$ solid solution, while at the same time Bi_2MoO_6 and $\text{Bi}_2\text{Mo}_3\text{O}_{12}$ emerged to maintain the stoichiometrics. This is supported by the EDS analysis as shown in Fig. 6. A small amount of Al element of about 2 mol% is observed in the thick films on Al foils sintered at 630°C (Fig. 6(b)), but is not detected in the compound sintered at 580°C (Fig. 6(c)).

Figure 3 is the SEM images of the thick films on Al foils with different sintering temperatures for 3 h. For the thick films sintered below 645°C , it shows the presence of pores and the number of pores decreases with increasing the sintering

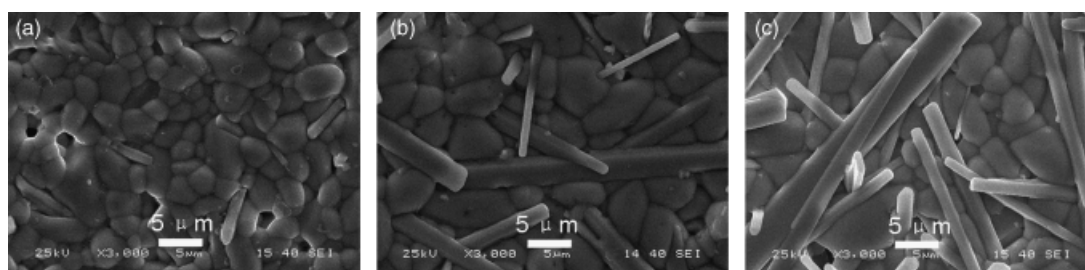


Fig. 7. Scanning electron microscope photos of $\text{Bi}_2\text{Mo}_2\text{O}_9$ thick films on Al foils sintered at 645°C for different dwell times: (a) 3 h, (b) 4 h, and (c) 5 h.

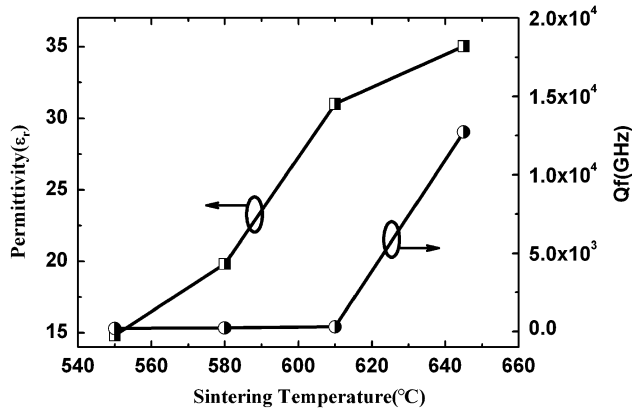


Fig. 10. Microwave dielectric properties of $\text{Bi}_2\text{Mo}_2\text{O}_9$ thick films on alumina substrates as a function of sintering temperature.

temperatures. The thick films sintered at 645°C for 3 h show a dense structure, which does improve the dielectric properties of the thick films. A plate-like secondary phase that appears at 620°C was approximately identified as Bi_2MoO_6 and $\text{Bi}_2\text{Mo}_3\text{O}_{12}$ by XRD (Fig. 1) and EDS analysis (Fig. 6(a)) with the atom ratio of Bi:Mo being about 1.8 (point 1). Figure 4 shows the similar morphologies of the thick films deposited on alumina substrates. Figure 5 presents the cross-section SEM image of $\text{Bi}_2\text{Mo}_2\text{O}_9/\text{Al}$ sample cofired at 645°C for 3 h in air. As observed in the micrograph, the $\text{Bi}_2\text{Mo}_2\text{O}_9$ thick film shows a dense microstructure and has a good contact with the Al electrode.

Figure 6(a) shows the EDS analysis of thick film on Al foils sintered at 645°C for 3 h, the sphere-like phase is the $\text{Bi}_2\text{Mo}_2\text{O}_9$ phase (point 3), and the plate-like phase is secondary phases (points 1 and 2). The SEM photos of $\text{Bi}_2\text{Mo}_2\text{O}_9$ thick films on Al foils sintered at 645°C for different dwell time are shown in Fig. 7. The secondary phases increase with the dwell time increasing from 3 to 5 h.

The frequency dependence of relative permittivity and dielectric loss of the thick films on Al foils are shown in Fig. 8. The relative permittivity and dielectric loss of the samples are strongly dependent on the sintering temperature. For the samples sintered at 550°C – 645°C , the relative permittivity increases remarkably from 15 to 38 with the sintering temperature increasing, while the dielectric loss decreases slightly. In addition, the frequency dependence of dielectric loss is lowered by increasing sintering temperatures. These results indicate that the dense and pore-free thick films possess better dielectric properties. The effect of secondary phase Bi_2MoO_6 and $\text{Bi}_2\text{Mo}_3\text{O}_{12}$ on dielectric properties could be neglected because these two compositions have the same dielectric properties and their content in the composite is too little. The dependence of dielectric proper-

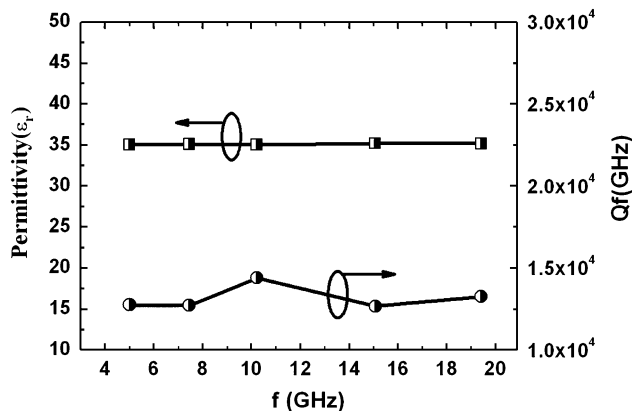


Fig. 11. Frequency dependence of microwave dielectric properties of $\text{Bi}_2\text{Mo}_2\text{O}_9$ thick films sintered at 645°C for 3 h on alumina substrates.

Table 1. The Value $\text{TC}\epsilon$ of the Thick Films on Alumina Substrate Sintered at Temperatures Ranging from 550° to 645°C for 3 h

Sintering temperature ($^\circ\text{C}$)	550	580	610	645
$\text{TC}\epsilon$ (ppm/ $^\circ\text{C}$)	17.8	15.2	34	124

ties on dwell time is shown in Fig. 9. The low frequency dependence of the relative permittivity and dielectric loss of the samples sintered at 645°C for different dwell times are observed. The relative permittivity shows a slight decrease from about 36 to 34.5 as the dwell time increases from 3 to 5 h. This could be ascribed to the phase assemblage change. As shown in Fig. 7, the secondary phases increase with the increasing dwell time. The secondary phases Bi_2MoO_6 and $\text{Bi}_2\text{Mo}_3\text{O}_{12}$ have slightly lower relative permittivities but the same dielectric losses when comparing with that of the $\text{Bi}_2\text{Mo}_2\text{O}_9$ phase.

The influence of sintering temperatures on microwave dielectric properties was measured at 5.011 GHz for the thick films on alumina substrates as shown in Fig. 10. It can be seen that the microwave relative permittivity and $Q \times f$ are strongly dependent on the sintering temperatures. When the sintering temperature increased from 550° to 645°C , the microwave relative permittivity increased from 15 to 35, and $Q \times f$ increased from 208 to 12 700 GHz. This is ascribed to a significant change in the microstructure of the thick films. As seen in Fig. 4, the microstructure of thick films on alumina substrates sintered at 645°C is denser than other samples. The frequency effects on the microwave relative permittivity and $Q \times f$ of the thick films sintered at 645°C for 3 h on alumina substrates are shown in Fig. 11. It is clear that the microwave dielectric properties are nearly frequency independent. The microwave relative permittivity is about 35, and the $Q \times f$ is about 12 500 GHz. The $\text{TC}\epsilon$ (τ_ϵ) value of the thick films as a function of sintering temperature is shown in Table I. The $\text{TC}\epsilon$ value increases from 17.8 to 124 ppm/ $^\circ\text{C}$ with the increasing sintering temperatures from 550° to 645°C for 3 h. In summary, the $\text{Bi}_2\text{Mo}_2\text{O}_9$ thick films show good microwave dielectric properties.

IV. Conclusions

Dense and pore-free $\text{Bi}_2\text{Mo}_2\text{O}_9$ thick films on Al foils and alumina substrates were prepared by screen-printing technology. The XRD analysis indicates that no second phase was detected in both the thick films on Al foils and alumina substrates when they were sintered at temperatures below 610°C . A small amount of secondary phases Bi_2MoO_6 and $\text{Bi}_2\text{Mo}_3\text{O}_{12}$ were observed in the thick films sintered at 610°C and higher temperatures. The effects of sintering temperature and dwell time on the relative permittivity and dielectric loss of the thick films have been studied. The sample sintered at 645°C for 3 h showed excellent dielectric properties. The relative permittivity is about 38 and the dielectric loss is about 0.7% in the frequency range from 1 kHz to 5 MHz. In the microwave frequency range from 5 GHz to 19 GHz, the relative permittivity of the thick films deposited on alumina substrates is 35, and the $Q \times f$ is about 12 500 GHz. The $\text{Bi}_2\text{Mo}_2\text{O}_9$ thick films obtained show potential application for LTCC device applications using Al electrode.

References

- Y.-J. Choi, J.-H. Park, and W.-J. Ko, "Low Temperature Sintering of BaTi_4O_9 -Based Middle-k Dielectric Composition for LTCC Applications," *J. Electroceram.*, **14**, 157–62 (2005).
- J.-H. Park, Y.-J. Choi, J.-H. Park, and J.-G. Park, "Low-Fire Dielectric Compositions with Permittivity," *Mater. Chem. Phys.*, **88**, 308–12 (2004).
- E. S. Kim, S. H. Kim, and B. I. Lee, "Low-Temperature Sintering and Microwave Dielectric Properties of CaWO_4 Ceramics for LTCC Applications," *J. Eur. Ceram. Soc.*, **26**, 2101–4 (2006).
- M. T. Sebastian and K. P. Surendran, "Tailoring the Microwave Dielectric Properties of $\text{Ba}(\text{Mg}_{1/3}\text{Ta}_{2/3})\text{O}_3$ Ceramics 20–60 for LTCC Applications," *J. Eur. Ceram. Soc.*, **26**, 1791–9 (2006).

⁵M. T. Sebastian and H. Jantunen, "Low Loss Dielectric Materials for LTCC Applications: A Review," *Int. Mater. Rev.*, **53**, 57–90 (2008).

⁶M. Udovic, M. Valant, and D. Suvorov, "Phase Formation and Dielectric Characterization of the Bi₂O₃–TeO₂ System Prepared in an Oxygen Atmosphere," *J. Am. Ceram. Soc.*, **87**, 591–7 (2004).

⁷M. Udovic, M. Valant, and D. Suvorov, "Dielectric Characterisation of Ceramics from the TiO₂–TeO₂ System," *J. Eur. Ceram. Soc.*, **21**, 1735–8 (2001).

⁸M. Valant and D. Suvorov, "Glass-Free Low-Temperature Co-Fired Ceramics: Calcium Germanates, Silicates and Tellurates," *J. Eur. Ceram. Soc.*, **24**, 1715–9 (2004).

⁹D. K. Kwon, M. T. Lanagan, and T. R. Shrout, "Microwave Dielectric Properties of BaO–TeO₂ Binary Compounds," *Mater. Lett.*, **61**, 1827–31 (2007).

¹⁰D. K. Kwon, M. T. Lanagan, and T. R. Shrout, "Microwave Dielectric Properties and Low-Temperature Cofiring of BaTe₄O₉ with Aluminum Metal Electrode," *J. Am. Ceram. Soc.*, **88**, 3419–22 (2005).

¹¹A. Feteira and D. C. Sinclair, "Microwave Dielectric Properties of Low Firing Temperature Bi₂W₂O₉ Ceramics," *J. Am. Ceram. Soc.*, **91**, 1338–41 (2008).

¹²D. Zhou, H. Wang, and X. Yao, "Microwave Dielectric Properties of Low Temperature Firing Bi₂Mo₂O₉ Ceramic," *J. Am. Ceram. Soc.*, **91**, 3419–22 (2008).

¹³J. Honkamo, H. Jantunen, G. Subodh, M. T. Sebastian, and P. Mohanan, "Tape Casting and Dielectric Properties of Zn₂Te₃O₈-Based Ceramics with an Ultra-Low Sintering Temperature," *Int. J. Appl. Ceram. Technol.*, **6**, 531–6 (2009).

¹⁴G. Subodh and M. T. Sebastian, "Glass-Free Zn₂Te₃O₈ Microwave Ceramic for LTCC Applications," *J. Am. Ceram. Soc.*, **90**, 2266–8 (2007).

¹⁵D. Zhou, C. A. Randall, H. Wang, L.-X. Pang, and X. Yao, "Dielectric Properties of a Ultra-Low Temperature Firing Bi₂Mo₂O₉ MLCCs Prepared by Tape-Casting," *J. Am. Ceram. Soc.*, (2010). doi: 10.1111/j.1551-2916.2010.03602.x.

¹⁶J. Krupka and W. Gwarrek, "Measurements and Modeling of Planar Metal Film Patterns Dielectric Substrates," *IEEE Microwave Wireless Comp. Lett.*, **19**, 134–6 (2009). □